
Towards Unsupervised Training of Matching-based Graph Edit Distance Solver via Preference-aware GAN

Wei Huang

University of New South Wales
 w.c.huang@unsw.edu.au

Hanchen Wang

University of Technology Sydney
 Hanchen.Wang@uts.edu.au

Dong Wen

University of New South Wales
 dong.wen@unsw.edu.au

Shaozhen Ma

University of New South Wales
 shaozhen.ma@unsw.edu.au

Wenjie Zhang

University of New South Wales
 wenjie.zhang@unsw.edu.au

Xuemin Lin

Shanghai Jiaotong University
 xuemin.lin@sjtu.edu.cn

Abstract

Graph Edit Distance (GED) is a fundamental graph similarity metric widely used in various applications. However, computing GED is an NP-hard problem. Recent state-of-the-art hybrid GED solver has shown promising performance by formulating GED as a bipartite graph matching problem, then leveraging a generative diffusion model to predict node matching between two graphs, from which both the GED and its corresponding edit path can be extracted using a traditional algorithm. However, such methods typically rely heavily on ground-truth supervision, where the ground-truth node matchings are often costly to obtain in real-world scenarios. In this paper, we propose GEDRanker, a novel unsupervised GAN-based framework for GED computation. Specifically, GEDRanker consists of a matching-based GED solver and introduces an interpretable preference-aware discriminator. By leveraging preference signals over different node matchings derived from edit path lengths, the discriminator can guide the matching-based solver toward generating high-quality node matching without the need for ground-truth supervision. Extensive experiments on benchmark datasets demonstrate that our GEDRanker enables the matching-based GED solver to achieve near-optimal solution quality without any ground-truth supervision. The source code is available at <https://github.com/piupiupiuu/GEDRanker>.

1 Introduction

Graph Edit Distance (GED) is a widely used graph similarity metric [1, 2, 3] that determines the minimum number of edit operations required to transform one graph into another. It has broad applications in domains such as pattern recognition [4, 5] and computer vision [6, 7]. Figure 1(a) illustrates an example of an optimal edit path for transforming G_1 to G_2 with $\text{GED}(G_1, G_2) = 4$. GED is particularly appealing due to its interpretability and its ability to capture both attribute-level and structural-level similarities between graphs. Traditional exact approaches for computing GED rely on A* search [8, 9, 10]. However, due to the NP-hardness of GED computation, these methods fail to scale to graphs with more than 16 nodes [9], making them impractical for large graphs.

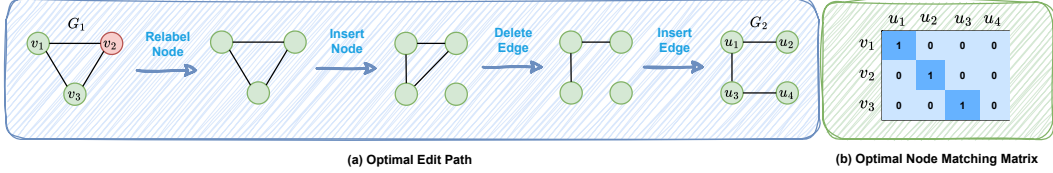


Figure 1: (a) An optimal edit path for converting G_1 to G_2 with $\text{GED}(G_1, G_2) = 4$. (b) An optimal node matching matrix from which an optimal edit path can be derived.

To address the limitations of traditional algorithms, hybrid approaches that combine deep learning with traditional algorithms have been widely explored. Recent hybrid approaches have focused on reformulating GED as a bipartite graph matching problem. Specifically, GEDGNN [11] and GEDIOT [12] propose to train a node matching model that predicts a single node matching probability matrix, where top- k edit paths can be extracted sequentially from the predicted matrices using a traditional algorithm. Later on, the current state-of-the-art GED solver, DiffGED [13], employs a generative diffusion model to predict top- k high quality node matching probability matrices in parallel, which parallelized the extraction of top- k edit paths. Notably, DiffGED has achieved near-optimal solution quality, closely approximating the ground-truth GED with a remarkable computational efficiency. Unfortunately, all existing hybrid GED solvers heavily rely on supervised learning, requiring ground-truth node matching matrices and GED values, which are often infeasible to obtain in practice due to the NP-hard nature of GED computation. This limits the usability of existing GED methods in real-world scenarios. Therefore, developing an unsupervised training framework for GED solvers is crucial for enhancing real-world applicability. Despite its importance, this direction remains largely underexplored.

In this paper, we propose GEDRanker, a novel GAN-based framework that enables the unsupervised training of a matching-based GED solver without relying on ground-truth node matching matrices. Unlike existing unsupervised training techniques commonly used in other problems, such as REINFORCE [14], GEDRanker provides a more effective and interpretable learning objective (*i.e.*, loss function) that enables GED solver to directly optimize a GED-related score. Specifically, we design an efficient unsupervised training strategy that incorporates a preference-aware discriminator. Rather than directly estimating the resulting edit path length of the node matching matrix, our preference-aware discriminator evaluates the preference over different node matching matrices, thereby providing richer feedback to guide the matching-based GED solver toward exploring high-quality solutions.

Contributions. To the best of our knowledge, GEDRanker is the first framework that enables unsupervised training of supervised neural methods for GED computation, offering a scalable and label-free alternative to supervised approaches. Experimental results on benchmark datasets show that the current state-of-the-art supervised matching-based GED solver, when trained under our unsupervised framework, achieves near-optimal solution quality comparable to supervised training with the same number of epochs, and outperforms all other supervised learning methods and traditional GED solvers.

2 Related Work

Traditional Approaches. Early approaches for solving GED are primarily based on exact combinatorial algorithms, such as A* search with handcrafted heuristics [9, 10]. While effective on small graphs, these methods are computationally prohibitive on larger graphs due to the NP-hardness of GED computation. To improve scalability, various approximate methods have been developed. These include bipartite matching formulations solved by the Hungarian algorithm [15] or the Volgenant-Jonker algorithm [16], as well as heuristic variants like A*-beam search [8] that limits the search space to enhance efficiency. However, such approximations often suffer from poor solution quality.

Deep Learning Approaches. More recently, deep learning methods have emerged as promising alternatives. SimGNN [17] and its successors [18, 19, 20, 21, 22, 23] formulate GED estimation as a regression task, enabling fast prediction of GED values. However, these methods do not recover the edit path, which is often critical in real applications. As a result, the predicted GED can be smaller than the true value, leading to infeasible solutions for which no valid edit path exists.

Hybrid Approaches. To address the limitations of regression-based deep learning methods, hybrid frameworks have been extensively studied to jointly estimate GED and recover the corresponding edit path. A class of approaches, including Noah [24], GENN-A* [25], and MATA* [26], integrate GNNs with A* search by generating dynamic heuristics or candidate matches. However, these methods still inherit the scalability bottlenecks of A*-based search. To improve both solution quality and computational efficiency, GEDGNN [11] and GEDIOT [12] reformulate GED estimation as a bipartite node matching problem. In this setting, a node matching model is trained to predict a node matching probability matrix, from which top- k edit paths are sequentially extracted using traditional algorithms. To further enhance solution quality and enable parallel extraction of top- k candidates, DiffGED [13], employs a generative diffusion-based node matching model to predict top- k node matching matrices in parallel, achieving near-optimal accuracy with significantly reduced running time. Motivated by its effectiveness and efficiency, we adopt the current state-of-the-art diffusion-based node matching model as the base GED solver of our unsupervised training framework.

3 Preliminaries

3.1 Problem Formulation

Problem Definition (Graph Edit Distance Computation). Given two graphs $G_1 = (V_1, E_1, L_1)$ and $G_2 = (V_2, E_2, L_2)$, where V , E and L represent the node set, edge set, and labeling function, respectively, we consider three types of edit operations: (1) Node insertion or deletion; (2) Edge insertion or deletion; (3) Node relabeling. An edit path is defined as a sequence of edit operations that transforms G_1 into G_2 . The Graph Edit Distance (GED) is the length of the optimal edit path that requires the minimum number of edit operations. In this paper, we aim not only to predict GED, but also to recover the corresponding edit path for the predicted GED.

Edit Path Generation. Given a pair of graphs G_1 and G_2 (assuming $|V_1| \leq |V_2|$), let $\pi \in \{0, 1\}^{|V_1| \times |V_2|}$ denote a binary node matching matrix that satisfy the following constraint:

$$\sum_{u=1}^{|V_2|} \pi[v][u] = 1 \quad \forall v \in V_1, \quad \sum_{v=1}^{|V_1|} \pi[v][u] \leq 1 \quad \forall u \in V_2 \quad (1)$$

where $\pi[v][u] = 1$ if node $v \in V_1$ is matched to node $u \in V_2$; otherwise $\pi[v][u] = 0$. Each $v \in V_1$ matches to exactly one $u \in V_2$, and each $u \in V_2$ matches to at most one $v \in V_1$. Given π , an edit path can be derived with a linear time complexity of $O(|V_2| + |E_1| + |E_2|)$ as follows:

(1) For each node $u \in V_2$, if u is matched to a node $v \in V_1$ and $L_1(v) \neq L_2(u)$, then relabel $L_1(v)$ to $L_2(u)$. If u is not matched to any node, then insert a new node with label $L_2(u)$ into V_1 , and match it to u . The overall time complexity of this step is $O(|V_2|)$.

(2) Suppose $v, v' \in V_1$ are matched to $u, u' \in V_2$, respectively. If $(v, v') \in E_1$ but $(u, u') \notin E_2$, then delete (v, v') from E_1 . If $(u, u') \in E_2$ but $(v, v') \notin E_1$, then insert (v, v') into E_1 . The overall time complexity of this step is $O(|E_1| + |E_2|)$.

Figure 1(b) shows an optimal node matching matrix from which the optimal edit path in Figure 1(a) is derived. Thus, computing GED can be reformulated as finding the optimal node matching matrix π^* that minimizes the total number of edit operations $c(G_1, G_2, \pi^*)$ in the resulting edit path.

Greedy Node Matching Matrix Decoding. Let $\hat{\pi} \in [0, 1]^{|V_1| \times |V_2|}$ be a node matching probability matrix, where $\hat{\pi}[v][u]$ denotes the matching probability between node v with node u . A binary node matching matrix π can be greedily decoded from $\hat{\pi}$ with a time complexity of $O(|V_1|^2 |V_2|)$ as follows:

- (1) Select node pair (v, u) with the highest probability in $\hat{\pi}$, and set $\pi[v][u] = 1$.
- (2) Set all values in the v -th row and u -th column of $\hat{\pi}$ to $-\infty$.
- (3) Repeat steps (1) and (2) for $|V_1|$ iterations.

Therefore, GED can be estimated by training a node matching model to generate node matching probability matrix that, when decoded, yields a node matching matrix minimizing the edit path length.

3.2 Supervised Diffusion-based Node Matching Model

The supervised diffusion-based node matching model [13] consists of a forward process and a reverse process. Intuitively, the forward process progressively corrupts the ground-truth node matching matrix π^* over T time steps to create a sequence of increasing noisy latent variables, such that $q(\pi^{1:T}|\pi^0) = \prod_{t=1}^T q(\pi^t|\pi^{t-1})$ with $\pi^0 = \pi^*$, where π^t with $t > 0$ is the noisy node matching matrix that does not need to satisfy the constraint defined in Equation 1. Next, a denoising network g_ϕ takes as input a graph pair (G_1, G_2) , a noisy matching matrix π^t , and the corresponding time step t , is trained to reconstruct π^* from π^t . During inference, the reverse process begins from a randomly sampled noisy matrix π^{t_S} , and iteratively applies g_ϕ to refine it towards a high-quality node matching matrix over a sequence of time steps $\{t_0, t_1, \dots, t_S\}$ with $S \leq T$, $t_0 = 0$ and $t_S = T$, such that $p_\theta(\pi^{t_0:t_S}|G_1, G_2) = p(\pi^{t_S}) \prod_{i=1}^S p_\theta(\pi^{t_{i-1}}|\pi^{t_i}, G_1, G_2)$.

Forward Process. Specifically, let $\tilde{\pi} \in \{0, 1\}^{|V_1| \times |V_2| \times 2}$ denote the one-hot encoding of a node matching matrix $\pi \in \{0, 1\}^{|V_1| \times |V_2|}$. The forward process corrupts π^{t-1} to π^t as: $q(\pi^t|\pi^{t-1}) = \text{Cat}(\pi^t|p = \tilde{\pi}^{t-1}Q_t)$, where $Q_t = \begin{bmatrix} 1 - \beta_t & \beta_t \\ \beta_t & 1 - \beta_t \end{bmatrix}$ is the transition probability matrix, Cat is the categorical distribution and β_t denotes the corruption ratio. The t -step marginal can be written as: $q(\pi^t|\pi^0) = \text{Cat}(\pi^t|p = \tilde{\pi}^0\bar{Q}_t)$, where $\bar{Q}_t = Q_1Q_2\dots Q_t$, this allows π^t to be sampled efficiently from π^0 during training.

Reverse Process. Starting from a randomly sampled noisy node matching matrix π^{t_S} , each step of the reverse process denoises π^{t_i} to $\pi^{t_{i-1}}$ as follows:

$$\begin{aligned} q(\pi^{t_{i-1}}|\pi^{t_i}, \pi^0) &= \frac{q(\pi^{t_i}|\pi^{t_{i-1}}, \pi^0)q(\pi^{t_{i-1}}|\pi^0)}{q(\pi^{t_i}|\pi^0)} \\ p_\phi(\tilde{\pi}^0|\pi^{t_i}, G_1, G_2) &= \sigma(g_\phi(G_1, G_2, \pi^{t_i}, t_i)) \\ p_\phi(\pi^{t_{i-1}}|\pi^{t_i}, G_1, G_2) &= \sum_{\tilde{\pi}} q(\pi^{t_{i-1}}|\pi^{t_i}, \tilde{\pi}^0)p_\phi(\tilde{\pi}^0|\pi^{t_i}, G_1, G_2) \\ \pi^{t_{i-1}} &\sim p_\phi(\pi^{t_{i-1}}|\pi^{t_i}, G_1, G_2) \end{aligned} \tag{2}$$

where $q(\pi^{t_{i-1}}|\pi^{t_i}, \pi^0)$ is the posterior, σ is the Sigmoid activation, and $p_\phi(\tilde{\pi}^0|\pi^{t_i}, G, G')$ is the node matching probabilities predicted by g_ϕ , the detailed architecture of g_ϕ is described in Appendix A.3.

During inference, for each reverse step except the final step, a binary noisy node matching matrix $\pi^{t_{i-1}}$ is sampled from $p_\phi(\pi^{t_{i-1}}|\pi^{t_i}, G_1, G_2)$ via Bernoulli sampling. For the final reverse step, we decode $p_\phi(\pi^0|\pi^{t_1}, G_1, G_2)$ following the greedy method described in Section 3.1 to obtain a constrained binary node matching matrix π^0 . The detailed procedure of reverse process can be found in Appendix A.1. To enhance the solution quality, k random initial π^{t_S} could be sampled in parallel, and k independent reverse processes could be performed in parallel to generate k candidate node matching matrices, the one results in the shortest edit path will be the final solution.

Supervised Training Strategy. In the supervised learning setting, at each training step, given a pair of graphs, a random time step t is sampled, and a noisy matching matrix π^t is sampled from $q(\pi^t|\pi^0)$, where $\pi^0 = \pi^*$ is the ground-truth optimal node matching matrix. The denoising network g_ϕ then takes as input a graph pair (G_1, G_2) , a noisy matching matrix π^t , and the time step t , and is trained to recover π^* from π^t by minimizing:

$$\mathcal{L}_{rec}(\pi^*) = \frac{1}{|V_1||V_2|} \sum_{v=1}^{|V_1|} \sum_{u=1}^{|V_2|} (\pi^*[v][u] \log(\hat{\pi}_{g_\phi}[v][u]) + (1 - \pi^*[v][u]) \log(1 - \sigma(\hat{\pi}_{g_\phi}[v][u]))) \tag{3}$$

where $\hat{\pi}_{g_\phi}$ is the node matching probability matrix such that: $\hat{\pi}_{g_\phi} = \sigma(g_\phi(G_1, G_2, \pi^t, t))$. However, this training strategy heavily relies on pre-computation of the ground-truth node matching matrix.

4 Proposed Approach: GEDRanker

4.1 Unsupervised Training Strategy

In practice, the ground-truth π^* is often unavailable, making it impractical to directly apply the supervised training strategy. Assuming the same set of training graphs as in the supervised learning

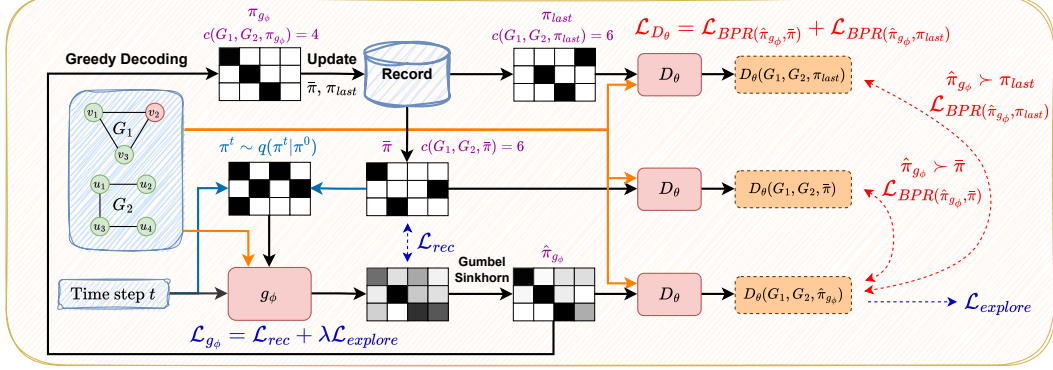


Figure 2: An overview of GEDRanker. For each training step, given a pair of training graphs, we maintain a record of the current best node matching matrix $\bar{\pi}$ and the node matching matrix obtained from the previous training step π_{last} . A noisy matching π^t is sampled at a random diffusion time step t and denoised by the denoising network g_ϕ to produce node matching scores. The resulting matching probability matrix $\hat{\pi}_{g_\phi}$ is obtained via Gumbel-Sinkhorn and greedily decoded to π_{g_ϕ} . The preference-aware discriminator D_θ is trained to learn a preference ordering over $\bar{\pi}$, π_{last} , and $\hat{\pi}_{g_\phi}$. Next, g_ϕ is trained to recover $\bar{\pi}$ and maximize the preference score $D_\theta(G_1, G_2, \hat{\pi}_{g_\phi})$. Finally, the record is updated by π_{g_ϕ} .

setting, a modified training strategy is to store a randomly initialized binary constrained node matching matrix as the current best solution $\bar{\pi}$ for each training graph pair. At each training step, for a given pair of graphs, we sample a random t , and sample a noisy matching matrix π^t from $q(\pi^t|\pi^0)$, with $\pi^0 = \bar{\pi}$, then g_ϕ is trained to recover $\bar{\pi}$ from π^t by minimizing $\mathcal{L}_{rec(\bar{\pi})}$. If the node matching matrix π_{g_ϕ} decoded from $\hat{\pi}_{g_\phi} = \sigma(g_\phi(G_1, G_2, \pi^t, t))$ yields a shorter edit path (i.e., $c(G_1, G_2, \pi_{g_\phi}) < c(G_1, G_2, \bar{\pi})$), then $\bar{\pi}$ is updated to π_{g_ϕ} . This guarantees that g_ϕ progressively finds a better solution during training, while recovering the current best solution.

However, the training objective in the above approach is fundamentally exploitative, as it only focused on recovering the currently best solution rather than actively exploring alternative solutions. While exploitation is beneficial in later stages when a high-quality solution is available, it is inefficient in the early stages of training, where the current best solution is likely far from optimal. In such cases, blindly recovering a suboptimal node matching matrix is ineffective and can mislead g_ϕ into poor learning directions, and hinder its ability to explore better solutions. Therefore, an effective training objective should prioritize exploring for better solutions in the early stages and shift its focus toward recovering high-quality solutions in the later stages.

RL-based Training Objective. A widely adopted strategy for guiding g_ϕ 's exploration towards better solutions is the use of reinforcement learning, specifically the REINFORCE [14], such that:

$$\nabla_\phi J(\phi) = \mathbb{E}_{\pi_{g_\phi}} [(c(G_1, G_2, \pi_{g_\phi}) - b) \nabla_\phi \log \sigma(g_\phi(\pi_{g_\phi} | G_1, G_2, \pi^t, t))] \quad (4)$$

where $c(G_1, G_2, \pi_{g_\phi})$ is the cost of the edit path computed according to the Edit Path Generation procedure in Section 3.1, and b is a baseline used to reduce gradient variance. This method adjusts the parameters of g_ϕ to increase or decrease the matching probability of each node pair based on the resulting edit path length, encouraging the model to generate node matching probability matrices that are more likely to yield shorter edit paths.

Unfortunately, this approach suffers from several limitations: (1) It does not directly optimize the graph edit distance and lacks interpretability, as the edit path length only serves as a scale for gradient updates; (2) It assumes all node pairs in π_{g_ϕ} contribute equally to the edit path length, thus all node pairs are assigned with the same scale, making it difficult to distinguish correctly predicted node matching probabilities from incorrect ones; (3) It ignores the combinatorial dependencies among node pairs, but the generated edit path is highly sensitive to such dependencies, limiting g_ϕ 's ability to efficiently explore high quality solutions.

GAN-based Training Objective. To overcome the limitations of REINFORCE, our GAN-based framework, GEDRanker, leverages a discriminator D_θ to guide g_ϕ 's exploration for better solutions. Specifically, given a node matching matrix π , the discriminator D_θ is trained to evaluate π and assign

Algorithm 1 Gumbel-Sinkhorn

a GED-related score $D_\theta(G_1, G_2, \pi)$. If π corresponds to a shorter edit path, then it will be assigned with a higher score; otherwise, a lower score. Therefore, g_ϕ is trained to maximize $D_\theta(G_1, G_2, \pi_{g_\phi})$.

However, the binary node matching matrix π_{g_ϕ} is greedily decoded from $\hat{\pi}_{g_\phi} = \sigma(g_\phi(G_1, G_2, \pi^t, t))$. This decoding process is non-differentiable, preventing g_ϕ from learning via gradient-based optimization. To address this issue, we employ the Gumbel-Sinkhorn method [27] to obtain a differentiable approximation of π_{g_ϕ} during training as outlined in Algorithm 1. Intuitively, Gumbel-Sinkhorn works by adding Gumbel noise to $g_\phi(G_1, G_2, \pi^t, t)$, followed by applying the Sinkhorn operator to produce a close approximation of a binary node matching matrix that satisfies the constraint defined in Equation 1. Let $S(\cdot)$ denote the Gumbel-Sinkhorn operation, we compute $\hat{\pi}_{g_\phi} = S(g_\phi(G_1, G_2, \pi^t, t))$ during training, and decode π_{g_ϕ} from $S(g_\phi(G_1, G_2, \pi^t, t))$ to generate the edit path, rather than decoding from $\sigma(g_\phi(G_1, G_2, \pi^t, t))$. Since $\hat{\pi}_{g_\phi}$ is now differentiable and closely approximates the decoded π_{g_ϕ} , we can now train g_θ to maximize $D_\theta(G_1, G_2, \hat{\pi}_{g_\phi})$ by minimizing the following loss:

$$\mathcal{L}_{explore} = -D_\theta(G_1, G_2, \hat{\pi}_{g_\phi}) = -D_\theta(G_1, G_2, S(g_\phi(G_1, G_2, \pi^t, t))) \quad (5)$$

Through this GAN-based approach, g_ϕ can directly optimize a GED-related score and provides interpretability. Moreover, the discriminator D_θ can learn to capture the dependencies between node pairs, and distinguish the influence of each predicted value in $\hat{\pi}_{g_\phi}$ on the generated edit path, thus can guide the training of g_ϕ in a more efficient way. Overall, g_ϕ is trained to minimize:

$$\mathcal{L}_{g_\phi} = \mathcal{L}_{rec(\bar{\pi})} + \lambda \mathcal{L}_{explore} \quad (6)$$

where λ is a hyperparameter that is dynamically decreased during training, encouraging exploration in the early stages and gradually shifting the focus toward exploitation in the later stages.

4.2 Discriminator

The discriminator D_θ is designed to assign a GED-related score to a given node matching matrix π based on a graph pair. What score should D_θ output?

A natural approach to train D_θ is to directly predict the resulting edit path length of π by minimizing the following loss:

$$\mathcal{L}_{\mathcal{D}_\theta} = (D_\theta(G_1, G_2, \pi) - \exp(-\frac{c(G_1, G_2, \pi) \times 2}{|V_1| + |V_2|}))^2 \quad (7)$$

where the edit path length is normalized by $\exp\left(-\frac{c(G_1, G_2, \pi) \times 2}{|V_1| + |V_2|}\right) \in (0, 1]$. Ideally, a shorter edit path should result in a higher score, allowing g_ϕ to learn to optimize the normalized GED. While this approach is straightforward and reasonable, can it guide g_ϕ towards the correct exploration direction?

Suppose we have two node matching matrices π_1 and π_2 , with $\exp(-\frac{c(G_1, G_2, \pi_1) \times 2}{|V_1| + |V_2|}) = 0.4$ and $\exp(-\frac{c(G_1, G_2, \pi_2) \times 2}{|V_1| + |V_2|}) = 0.6$. Considering two cases, in Case 1, we have $D_\theta(G_1, G_2, \pi_1) = 0.1$ and $D_\theta(G_1, G_2, \pi_2) = 0.9$, resulting in $\mathcal{L}_{\mathcal{D}_\theta} = 0.18$. In Case 2, we have $D_\theta(G_1, G_2, \pi_1) = 0.6$ and $D_\theta(G_1, G_2, \pi_2) = 0.4$, resulting in $\mathcal{L}_{\mathcal{D}_\theta} = 0.08$. Clearly, Case 2 is preferred by D_θ due to the lower $\mathcal{L}_{\mathcal{D}_\theta}$. Consequently, based on the interpretable $\mathcal{L}_{\text{explore}}$, g_ϕ would be encouraged to generate π_1 over π_2 as it results in a lower loss. However, π_1 actually corresponds to a longer edit path, meaning that

the exploration direction of g_ϕ is misled by D_θ , and such case would happen frequently when D_θ is not well trained. Thus, what matters for D_θ is not learning the precise normalized edit path length, but rather ensuring the correct preference ordering over different π .

Preference-aware Training Objective. To ensure that D_θ learns the correct preference, we introduce a preference-aware discriminator. A node matching matrix with a shorter edit path should be preferred (\succ) over one with a longer edit path. The objective of the preference-aware discriminator is to guarantee that the score assigned to the preferred node matching matrix is ranked higher than that of the less preferred one. Specifically, at each training step, given a pair of graphs, we have the current best node matching matrix $\bar{\pi}$ and the predicted node matching probability matrix $\hat{\pi}_{g_\phi} = S(g_\phi(G_1, G_2, \pi^t, t))$. The preference-aware discriminator is trained to minimize the following Bayes Personalized Ranking (BPR) loss [28]:

$$\mathcal{L}_{BPR}(\hat{\pi}_{g_\phi}, \bar{\pi}) = \begin{cases} -\log \sigma(D_\theta(G_1, G_2, \hat{\pi}_{g_\phi}) - D_\theta(G_1, G_2, \bar{\pi})) & \text{if } c(G_1, G_2, \hat{\pi}_{g_\phi}) \leq c(G_1, G_2, \bar{\pi}) \\ -\log \sigma(D_\theta(G_1, G_2, \bar{\pi}) - D_\theta(G_1, G_2, \hat{\pi}_{g_\phi})) & \text{if } c(G_1, G_2, \hat{\pi}_{g_\phi}) \geq c(G_1, G_2, \bar{\pi}) \end{cases} \quad (8)$$

BPR encourages the preference-aware discriminator to increase the preference score of the better node matching matrix while simultaneously decreasing the preference score of the worse one, thereby promoting a clear separation between high and low quality solutions. Note that, other ranking loss functions, such as Hinge Loss, could be an alternative. Now, Case 1 yields a lower loss of $\mathcal{L}_{BPR}(\pi_1, \pi_2) = 0.3711$, whereas Case 2 results in a higher loss of $\mathcal{L}_{BPR}(\pi_1, \pi_2) = 0.7981$. Consequently, D_θ would choose Case 1, and g_ϕ would be encouraged to generate π_2 over π_1 . Notably, for the special case where $c(G_1, G_2, \hat{\pi}_{g_\phi}) = c(G_1, G_2, \bar{\pi})$, $\mathcal{L}_{BPR}(\hat{\pi}_{g_\phi}, \bar{\pi})$ is computed in both directions to ensure that the loss is minimized only if $\hat{\pi}_{g_\phi}$ and $\bar{\pi}$ are assigned with the same preference score.

Moreover, finding a better solution becomes increasingly challenging as training progresses. Consequently, $\bar{\pi}$ is updated less frequently in later training stages, leading to a scenario where a single node matching matrix may dominate $\bar{\pi}$. In this case, the discriminator can only learn to rank $\hat{\pi}_{g_\phi}$ against this specific $\bar{\pi}$, but may fail to correctly rank $\hat{\pi}_{g_\phi}$ against other node matching matrices. To deal with such case, we store an additional historical node matching matrix π_{last} decoded from $\hat{\pi}_{g_\phi}$ in the previous training step. We then compute an additional ranking loss $\mathcal{L}_{BPR}(\hat{\pi}_{g_\phi}, \pi_{last})$ to encourage a more robust ranking mechanism. Overall, the discriminator is trained to minimize the following loss:

$$\mathcal{L}_{D_\theta} = \mathcal{L}_{BPR}(\hat{\pi}_{g_\phi}, \bar{\pi}) + \mathcal{L}_{BPR}(\hat{\pi}_{g_\phi}, \pi_{last}) \quad (9)$$

The overall framework of GEDRanker is illustrated in Figure 2 and outlined in Algorithm 3.

Discriminator Architecture. To effectively capture the dependencies among node pairs and distinguish the influence of each predicted node matching on the resulting edit path, our D_θ leverages GIN [29] and Anisotropic Graph Neural Network (AGNN) [30, 31, 32] to compute the embeddings of each node pair, then estimates the preference score directly based on these embeddings. Due to the space limitation, more details about the architecture of D_θ can be found in Appendix A.3 and C.3.

5 Experiments

5.1 Experimental Settings

Datasets. We conduct experiments on three widely used real world datasets: AIDS700 [17], Linux [33, 17], and IMDB [17, 34]. Each dataset is split into 60%, 20% and 20% as training graphs, validation graphs and testing graphs, respectively. We construct training, validation, and testing graph pairs, and generate their corresponding ground-truth GEDs and node matching matrices for evaluation following the strategy described in [11]. More details of the datasets can be found in Appendix B.1.

Baselines. We categorize baseline methods and our GEDRanker into three groups: (1) Traditional approximation methods: Hungarian [15], VJ [16] and GEDGW [12]; (2) Supervised hybrid methods: Noah [24], GENN-A* [25], MATA* [26], GEDGNN [11], GEDIOT [12] and DiffGED [13]; (3) Unsupervised hybrid method: GEDRanker. Due to the space limitations, the implementation details of our GEDRanker could be found in Appendix B.2.

Evaluation Metrics. We evaluate the performance of each model using the following metrics: (1) *Mean Absolute Error* (MAE) measures average absolute error between the predicted GED and

Table 1: Overall performance on testing graph pairs. Methods with a running time exceeding 24 hours are marked with -. \uparrow : higher is better. \downarrow : lower is better. **Bold**: best in its own group. Trad, SL and UL denotes Traditional, Supervised Learning and Unsupervised Learning, respectively. Results for baselines, except for GEDIOT and GEDGW, are taken from [13].

Datasets	Models	Type	MAE \downarrow	Accuracy \uparrow	$\rho \uparrow$	$\tau \uparrow$	$p@10 \uparrow$	$p@20 \uparrow$	Time(s) \downarrow
AIDS700	Hungarian	Trad	8.247	1.1%	0.547	0.431	52.8%	59.9%	0.00011
	VJ	Trad	14.085	0.6%	0.372	0.284	41.9%	52%	0.00017
	GEDGW	Trad	0.811	53.9%	0.866	0.78	84.9%	85.7%	0.39255
	Noah	SL	3.057	6.6%	0.751	0.629	74.1%	76.9%	0.6158
	GENN-A*	SL	0.632	61.5%	0.903	0.815	85.6%	88%	2.98919
	MATA*	SL	0.838	58.7%	0.8	0.718	73.6%	77.6%	0.00487
	GEDGNN	SL	1.098	52.5%	0.845	0.752	89.1%	88.3%	0.39448
	GEDIOT	SL	1.188	53.5%	0.825	0.73	88.6%	86.7%	0.39357
	DiffGED	SL	0.022	98%	0.996	0.992	99.8%	99.7%	0.0763
Linux	GEDRanker (Ours)	UL	0.088	92.6%	0.984	0.969	99.1%	99.1%	0.0759
	Hungarian	Trad	5.35	7.4%	0.696	0.605	74.8%	79.6%	0.00009
	VJ	Trad	11.123	0.4%	0.594	0.5	72.8%	76%	0.00013
	GEDGW	Trad	0.532	75.4%	0.919	0.864	90.5%	92.2%	0.1826
	Noah	SL	1.596	9%	0.9	0.834	92.6%	96%	0.24457
	GENN-A*	SL	0.213	89.4%	0.954	0.905	99.1%	98.1%	0.68176
	MATA*	SL	0.18	92.3%	0.937	0.893	88.5%	91.8%	0.00464
	GEDGNN	SL	0.094	96.6%	0.979	0.969	98.9%	99.3%	0.12863
	GEDIOT	SL	0.117	95.3%	0.978	0.966	98.8%	99%	0.13535
IMDB	DiffGED	SL	0.0	100%	1.0	1.0	100%	100%	0.06982
	GEDRanker (Ours)	UL	0.01	99.5%	0.997	0.995	100%	99.8%	0.06973
	Hungarian	Trad	21.673	45.1%	0.778	0.716	83.8%	81.9%	0.0001
	VJ	Trad	44.078	26.5%	0.4	0.359	60.1%	62%	0.00038
	GEDGW	Trad	0.349	93.9%	0.966	0.953	99.1%	98.3%	0.37496
	Noah	SL	-	-	-	-	-	-	-
	GENN-A*	SL	-	-	-	-	-	-	-
	MATA*	SL	-	-	-	-	-	-	-
	GEDGNN	SL	2.469	85.5%	0.898	0.879	92.4%	92.1%	0.42428
IMDB	GEDIOT	SL	2.822	84.5%	0.9	0.878	92.3%	92.7%	0.41959
	DiffGED	SL	0.937	94.6%	0.982	0.973	97.5%	98.3%	0.15105
IMDB	GEDRanker (Ours)	UL	1.019	94%	0.999	0.97	96.1%	97%	0.15111

the ground-truth GED; (2) *Accuracy* measures the proportion of test pairs whose predicted GED equals the ground-truth GED; (3) *Spearman’s Rank Correlation Coefficient* (ρ), and (4) *Kendall’s Rank Correlation Coefficient* (τ) both measure the matching ratio between the ranking results of the predicted GED and the ground-truth GED for each query test graph; (5) *Precision at 10/20* ($p@10$, $p@20$) measures the proportion of predicted top-10/20 most similar graphs that appear in the ground-truth top-10/20 similar graphs for each query test graph. (6) *Time (s)* measures the average running time of each test graph pair.

5.2 Main Results

Table 1 presents the overall performance of each method on the test graph pairs. Among supervised methods, the diffusion-based node matching model DiffGED achieves near-optimal accuracy across all datasets. Our unsupervised GEDRanker, which trains diffusion-based node matching model without ground-truth labels but with the same number of training epochs, also outperforms other supervised methods and achieves near-optimal solution quality, with an insignificant performance gap compared to DiffGED.

Furthermore, compared to the traditional approximation method GEDGW, GEDRanker consistently achieves higher solution quality while maintaining shorter running times across all datasets. It is worth noting that on the IMDB dataset, GEDGW exhibits a lower MAE, this is because IMDB contains synthetic large graph pairs, where approximated ground-truth GED values might be higher than the actual ground-truth GED values. As a result, a lower MAE only reflects the predicted GED values are close to the approximated ground-truth values.

Table 2: Ablation study.

Datasets	Models	MAE \downarrow	Accuracy \uparrow	$\rho \uparrow$	$\tau \uparrow$	$p@10 \uparrow$	$p@20 \uparrow$
AIDS700	GEDRanker (plain)	0.549	65.4%	0.905	0.837	91.7%	91.5%
	GEDRanker (RL)	0.458	69.3%	0.921	0.86	91.1%	92.7%
	GEDRanker (GED)	0.237	82.3%	0.956	0.919	97.6%	96.5%
	GEDRanker (Hinge)	0.114	90.5%	0.98	0.96	98.9%	98.6%
	GEDRanker	0.088	92.6%	0.984	0.969	99.1%	99.1%
Linux	GEDRanker (plain)	0.079	96.2%	0.984	0.973	98.1%	98.3%
	GEDRanker (RL)	0.04	98%	0.99	0.984	99.2%	99.2%
	GEDRanker (GED)	0.017	99.2%	0.995	0.992	99.4%	99.6%
	GEDRanker (Hinge)	0.002	99.9%	0.999	0.999	100%	100%
	GEDRanker	0.01	99.5%	0.997	0.995	100%	99.8%

5.3 Ablation Study

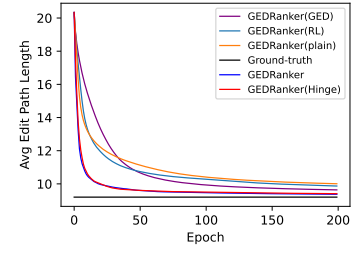
Exploration Ability. To evaluate the significant of the exploration during unsupervised learning as well as the exploration ability of our proposed GEDRanker, we create three variant models: (1) *GEDRanker (plain)*, which simply trains g_ϕ only to recover the current best solution using $\mathcal{L}_{rec}(\pi)$ without any exploration; (2) *GEDRanker (RL)*, which guides g_ϕ ’s exploration using REINFORCE by replacing $\mathcal{L}_{explore}$ with Equation 4; (3) *GEDRanker (GED)*, which replaces the preference-aware discriminator with a discriminator that directly estimates the edit path length (Equation 7).

Table 2 presents the performance of each variant model on testing graph pairs. The results show that the performance of GEDRanker (plain) drops significantly without exploration, indicating that a purely exploitative approach focused solely on recovering the current best solution is insufficient. Furthermore, Figure 3 shows the average edit path length of the best found solutions on training graph pairs. Obviously, GEDRanker (plain) exhibits the weakest ability to discover better solutions, which misleads g_ϕ into recovering suboptimal solutions.

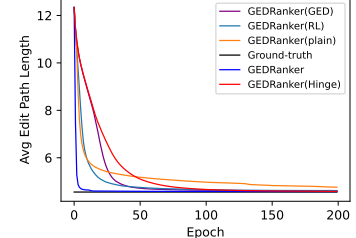
For the variant models that incorporate exploration, GEDRanker (RL), which guides the exploration of g_ϕ using REINFORCE, slightly improves the overall performance and exploration ability compared to GEDRanker (plain) as demonstrated in Table 2 and Figure 3. However, there still remains a significant performance gap compared to our GAN-based approaches GEDRanker and GEDRanker (GED). This gap arises because REINFORCE cannot directly optimize GED and struggles to capture the dependencies among node pairs as well as the individual impact of each node pair on the resulting edit path, whereas our GAN-based framework is able to capture both effectively.

Moreover, the preference-aware discriminator used in GEDRanker further enhances the exploration ability, compared to the discriminator used in GEDRanker (GED) that directly estimates the edit path length. As shown in Figure 3, the average edit path length of the best solution found by GEDRanker converges to a near-optimal value significantly faster than all variant models, indicating a strong ability to explore for high quality solutions. Consequently, this allows g_ϕ more epochs to recover high quality solutions, thereby improving the overall performance, as demonstrated in Table 2.

In contrast, GEDRanker (GED) struggles to identify better solutions during the early training phase. This observation aligns with our earlier analysis: a discriminator that directly estimates edit path length may produce incorrect preferences over different π when D_θ is not yet well-trained, thereby misguiding the exploration direction of g_ϕ . As training progresses, the edit path estimation becomes more accurate, such incorrect preference occurs less frequently, thus its exploration ability becomes better than GEDRanker (plain) and GEDRanker (RL).



(a) AIDS700



(b) Linux

Figure 3: Average edit path length of the best found node matching matrices on training graph pairs.

Ranking Loss. For the preference-aware discriminator, we adopt the BPR ranking loss. To evaluate the effect of alternative ranking loss, we introduce a variant model, *GEDRanker (Hinge)*, which replaces BPR with a Hinge loss to rank the preference over different node matching matrices π . Following the same setting as in Equation 8, the Hinge loss is computed with a margin of 1 when the two node matching matrices yield different edit path lengths, and with a margin of 0 when they result in the same edit path length. In the latter case, the loss is computed in both directions to encourage their predicted scores to be as similar as possible. The detailed Hinge loss is shown in Appendix A.4.

The overall performance of GEDRanker (Hinge) is very close to that of GEDRanker with BPR loss, and both outperform all non-preference-aware variants, as shown in Table 2, further validating the effectiveness of our proposed preference-aware discriminator. However, as shown in Figure 3, the exploration ability of GEDRanker (Hinge) is less stable compared to GEDRanker. On the AIDS700 dataset, they both exhibit similar exploration trends, while on the Linux dataset, GEDRanker (Hinge) performs poorly during the early training phase. This discrepancy arises because Hinge loss produces non-smooth, discontinuous gradients, and it is sensitive to the choice of margin, making optimization less stable. Therefore, we choose to adopt BPR loss for our preference-aware discriminator.

6 Conclusion

In this paper, we propose GEDRanker, the first unsupervised training framework for GED computation. Specifically, GEDRanker adopts a GAN-based design, consisting of a node matching-based GED solver and a preference-aware discriminator that evaluates the relative quality of different node matching matrices. Extensive experiments on benchmark datasets demonstrate that GEDRanker enables the current state-of-the-art supervised GED solver to achieve near-optimal performance under a fully unsupervised setting, while also outperforming all other supervised and traditional baselines.

Acknowledgments

Hanchen Wang is supported by ARC DE250100226. Dong Wen is supported by ARC DP230101445 and ARC DE240100668.

References

- [1] K. Gouda and M. Arafa, “An improved global lower bound for graph edit similarity search,” *Pattern Recognition Letters*, vol. 58, pp. 8–14, 2015.
- [2] Y. Liang and P. Zhao, “Similarity search in graph databases: A multi-layered indexing approach,” in *2017 IEEE 33rd International Conference on Data Engineering (ICDE)*. IEEE, 2017, pp. 783–794.
- [3] H. Bunke, “On a relation between graph edit distance and maximum common subgraph,” *Pattern recognition letters*, vol. 18, no. 8, pp. 689–694, 1997.
- [4] P. Maergner, V. Pondenkandath, M. Alberti, M. Liwicki, K. Riesen, R. Ingold, and A. Fischer, “Combining graph edit distance and triplet networks for offline signature verification,” *Pattern Recognition Letters*, vol. 125, pp. 527–533, 2019.
- [5] H. Bunke and G. Allermann, “Inexact graph matching for structural pattern recognition,” *Pattern Recognition Letters*, vol. 1, no. 4, pp. 245–253, 1983.
- [6] M. Cho, K. Alahari, and J. Ponce, “Learning graphs to match,” in *Proceedings of the IEEE International Conference on Computer Vision*, 2013, pp. 25–32.
- [7] L. Chen, G. Lin, S. Wang, and Q. Wu, “Graph edit distance reward: Learning to edit scene graph,” in *Computer Vision–ECCV 2020: 16th European Conference, Glasgow, UK, August 23–28, 2020, Proceedings, Part XIX 16*. Springer, 2020, pp. 539–554.
- [8] M. Neuhaus, K. Riesen, and H. Bunke, “Fast suboptimal algorithms for the computation of graph edit distance,” in *Structural, Syntactic, and Statistical Pattern Recognition: Joint IAPR International Workshops, SSPR 2006 and SPR 2006, Hong Kong, China, August 17–19, 2006. Proceedings*. Springer, 2006, pp. 163–172.
- [9] D. B. Blumenthal and J. Gamper, “On the exact computation of the graph edit distance,” *Pattern Recognition Letters*, vol. 134, pp. 46–57, 2020.

- [10] L. Chang, X. Feng, X. Lin, L. Qin, W. Zhang, and D. Ouyang, “Speeding up ged verification for graph similarity search,” in *2020 IEEE 36th International Conference on Data Engineering (ICDE)*. IEEE, 2020, pp. 793–804.
- [11] C. Piao, T. Xu, X. Sun, Y. Rong, K. Zhao, and H. Cheng, “Computing graph edit distance via neural graph matching,” *Proceedings of the VLDB Endowment*, vol. 16, no. 8, pp. 1817–1829, 2023.
- [12] Q. Cheng, D. Yan, T. Wu, Z. Huang, and Q. Zhang, “Computing approximate graph edit distance via optimal transport,” *Proceedings of the ACM on Management of Data*, vol. 3, no. 1, pp. 1–26, 2025.
- [13] W. Huang, H. Wang, D. Wen, W. Zhang, Y. Zhang, and X. Lin, “Diffged: Computing graph edit distance via diffusion-based graph matching,” *arXiv preprint arXiv:2503.18245*, 2025.
- [14] R. J. Williams, “Simple statistical gradient-following algorithms for connectionist reinforcement learning,” *Machine learning*, vol. 8, pp. 229–256, 1992.
- [15] K. Riesen and H. Bunke, “Approximate graph edit distance computation by means of bipartite graph matching,” *Image and Vision computing*, vol. 27, no. 7, pp. 950–959, 2009.
- [16] H. Bunke, K. Riesen, and S. Fankhauser, “Speeding up graph edit distance computation through fast bipartite matching,” 2011.
- [17] Y. Bai, H. Ding, S. Bian, T. Chen, Y. Sun, and W. Wang, “Simgnn: A neural network approach to fast graph similarity computation,” in *Proceedings of the twelfth ACM international conference on web search and data mining*, 2019, pp. 384–392.
- [18] J. Bai and P. Zhao, “Tagsim: Type-aware graph similarity learning and computation,” *Proceedings of the VLDB Endowment*, vol. 15, no. 2, 2021.
- [19] W. Zhuo and G. Tan, “Efficient graph similarity computation with alignment regularization,” *Advances in Neural Information Processing Systems*, vol. 35, pp. 30 181–30 193, 2022.
- [20] X. Ling, L. Wu, S. Wang, T. Ma, F. Xu, A. X. Liu, C. Wu, and S. Ji, “Multilevel graph matching networks for deep graph similarity learning,” *IEEE Transactions on Neural Networks and Learning Systems*, vol. 34, no. 2, pp. 799–813, 2021.
- [21] Y. Bai, H. Ding, K. Gu, Y. Sun, and W. Wang, “Learning-based efficient graph similarity computation via multi-scale convolutional set matching,” in *Proceedings of the AAAI conference on artificial intelligence*, vol. 34, no. 04, 2020, pp. 3219–3226.
- [22] Z. Zhang, J. Bu, M. Ester, Z. Li, C. Yao, Z. Yu, and C. Wang, “H2mn: Graph similarity learning with hierarchical hypergraph matching networks,” in *Proceedings of the 27th ACM SIGKDD conference on knowledge discovery & data mining*, 2021, pp. 2274–2284.
- [23] C. Qin, H. Zhao, L. Wang, H. Wang, Y. Zhang, and Y. Fu, “Slow learning and fast inference: Efficient graph similarity computation via knowledge distillation,” *Advances in Neural Information Processing Systems*, vol. 34, pp. 14 110–14 121, 2021.
- [24] L. Yang and L. Zou, “Noah: Neural-optimized a* search algorithm for graph edit distance computation,” in *2021 IEEE 37th International Conference on Data Engineering (ICDE)*. IEEE, 2021, pp. 576–587.
- [25] R. Wang, T. Zhang, T. Yu, J. Yan, and X. Yang, “Combinatorial learning of graph edit distance via dynamic embedding,” in *Proceedings of the IEEE/CVF Conference on Computer Vision and Pattern Recognition*, 2021, pp. 5241–5250.
- [26] J. Liu, M. Zhou, S. Ma, and L. Pan, “Mata*: Combining learnable node matching with a* algorithm for approximate graph edit distance computation,” in *Proceedings of the 32nd ACM International Conference on Information and Knowledge Management*, 2023, pp. 1503–1512.
- [27] G. Mena, D. Belanger, S. Linderman, and J. Snoek, “Learning latent permutations with gumbel-sinkhorn networks,” *arXiv preprint arXiv:1802.08665*, 2018.
- [28] S. Rendle, C. Freudenthaler, Z. Gantner, and L. Schmidt-Thieme, “Bpr: Bayesian personalized ranking from implicit feedback,” *arXiv preprint arXiv:1205.2618*, 2012.
- [29] K. Xu, W. Hu, J. Leskovec, and S. Jegelka, “How powerful are graph neural networks?” *arXiv preprint arXiv:1810.00826*, 2018.
- [30] C. K. Joshi, Q. Cappart, L.-M. Rousseau, and T. Laurent, “Learning the travelling salesperson problem requires rethinking generalization,” *arXiv preprint arXiv:2006.07054*, 2020.

- [31] Z. Sun and Y. Yang, “Difusco: Graph-based diffusion solvers for combinatorial optimization,” *Advances in Neural Information Processing Systems*, vol. 36, pp. 3706–3731, 2023.
- [32] R. Qiu, Z. Sun, and Y. Yang, “Dimes: A differentiable meta solver for combinatorial optimization problems,” *Advances in Neural Information Processing Systems*, vol. 35, pp. 25 531–25 546, 2022.
- [33] X. Wang, X. Ding, A. K. Tung, S. Ying, and H. Jin, “An efficient graph indexing method,” in *2012 IEEE 28th International Conference on Data Engineering*. IEEE, 2012, pp. 210–221.
- [34] P. Yanardag and S. Vishwanathan, “Deep graph kernels,” in *Proceedings of the 21th ACM SIGKDD international conference on knowledge discovery and data mining*, 2015, pp. 1365–1374.
- [35] A. Vaswani, N. Shazeer, N. Parmar, J. Uszkoreit, L. Jones, A. N. Gomez, Ł. Kaiser, and I. Polosukhin, “Attention is all you need,” *Advances in neural information processing systems*, vol. 30, 2017.
- [36] T. Cai, S. Luo, K. Xu, D. He, T.-y. Liu, and L. Wang, “Graphnorm: A principled approach to accelerating graph neural network training,” in *International Conference on Machine Learning*. PMLR, 2021, pp. 1204–1215.

NeurIPS Paper Checklist

1. Claims

Question: Do the main claims made in the abstract and introduction accurately reflect the paper's contributions and scope?

Answer: [\[Yes\]](#)

Justification: Yes, the main claims made in the abstract and introduction accurately reflect the paper's contributions and scope. The key contributions are clearly described at the end of both the abstract and introduction. These contributions are thoroughly elaborated in Section 4 and Appendix A, and validated through extensive experiments presented in Section 5 and Appendix C.

Guidelines:

- The answer NA means that the abstract and introduction do not include the claims made in the paper.
- The abstract and/or introduction should clearly state the claims made, including the contributions made in the paper and important assumptions and limitations. A No or NA answer to this question will not be perceived well by the reviewers.
- The claims made should match theoretical and experimental results, and reflect how much the results can be expected to generalize to other settings.
- It is fine to include aspirational goals as motivation as long as it is clear that these goals are not attained by the paper.

2. Limitations

Question: Does the paper discuss the limitations of the work performed by the authors?

Answer: [\[Yes\]](#)

Justification: Yes, we have discussed the limitations of this work in Appendix D.

Guidelines:

- The answer NA means that the paper has no limitation while the answer No means that the paper has limitations, but those are not discussed in the paper.
- The authors are encouraged to create a separate "Limitations" section in their paper.
- The paper should point out any strong assumptions and how robust the results are to violations of these assumptions (e.g., independence assumptions, noiseless settings, model well-specification, asymptotic approximations only holding locally). The authors should reflect on how these assumptions might be violated in practice and what the implications would be.
- The authors should reflect on the scope of the claims made, e.g., if the approach was only tested on a few datasets or with a few runs. In general, empirical results often depend on implicit assumptions, which should be articulated.
- The authors should reflect on the factors that influence the performance of the approach. For example, a facial recognition algorithm may perform poorly when image resolution is low or images are taken in low lighting. Or a speech-to-text system might not be used reliably to provide closed captions for online lectures because it fails to handle technical jargon.
- The authors should discuss the computational efficiency of the proposed algorithms and how they scale with dataset size.
- If applicable, the authors should discuss possible limitations of their approach to address problems of privacy and fairness.
- While the authors might fear that complete honesty about limitations might be used by reviewers as grounds for rejection, a worse outcome might be that reviewers discover limitations that aren't acknowledged in the paper. The authors should use their best judgment and recognize that individual actions in favor of transparency play an important role in developing norms that preserve the integrity of the community. Reviewers will be specifically instructed to not penalize honesty concerning limitations.

3. Theory assumptions and proofs

Question: For each theoretical result, does the paper provide the full set of assumptions and a complete (and correct) proof?

Answer: [NA]

Justification: The paper does not include theoretical results.

Guidelines:

- The answer NA means that the paper does not include theoretical results.
- All the theorems, formulas, and proofs in the paper should be numbered and cross-referenced.
- All assumptions should be clearly stated or referenced in the statement of any theorems.
- The proofs can either appear in the main paper or the supplemental material, but if they appear in the supplemental material, the authors are encouraged to provide a short proof sketch to provide intuition.
- Inversely, any informal proof provided in the core of the paper should be complemented by formal proofs provided in appendix or supplemental material.
- Theorems and Lemmas that the proof relies upon should be properly referenced.

4. Experimental result reproducibility

Question: Does the paper fully disclose all the information needed to reproduce the main experimental results of the paper to the extent that it affects the main claims and/or conclusions of the paper (regardless of whether the code and data are provided or not)?

Answer: [Yes]

Justification: Our paper fully disclose all the information needed to reproduce the main experimental results, the details of implementations and experimental settings can be found in Section 5.1 and Appendix B. We also provide the code and data in supplementary materials.

Guidelines:

- The answer NA means that the paper does not include experiments.
- If the paper includes experiments, a No answer to this question will not be perceived well by the reviewers: Making the paper reproducible is important, regardless of whether the code and data are provided or not.
- If the contribution is a dataset and/or model, the authors should describe the steps taken to make their results reproducible or verifiable.
- Depending on the contribution, reproducibility can be accomplished in various ways. For example, if the contribution is a novel architecture, describing the architecture fully might suffice, or if the contribution is a specific model and empirical evaluation, it may be necessary to either make it possible for others to replicate the model with the same dataset, or provide access to the model. In general, releasing code and data is often one good way to accomplish this, but reproducibility can also be provided via detailed instructions for how to replicate the results, access to a hosted model (e.g., in the case of a large language model), releasing of a model checkpoint, or other means that are appropriate to the research performed.
- While NeurIPS does not require releasing code, the conference does require all submissions to provide some reasonable avenue for reproducibility, which may depend on the nature of the contribution. For example
 - (a) If the contribution is primarily a new algorithm, the paper should make it clear how to reproduce that algorithm.
 - (b) If the contribution is primarily a new model architecture, the paper should describe the architecture clearly and fully.
 - (c) If the contribution is a new model (e.g., a large language model), then there should either be a way to access this model for reproducing the results or a way to reproduce the model (e.g., with an open-source dataset or instructions for how to construct the dataset).
 - (d) We recognize that reproducibility may be tricky in some cases, in which case authors are welcome to describe the particular way they provide for reproducibility. In the case of closed-source models, it may be that access to the model is limited in

some way (e.g., to registered users), but it should be possible for other researchers to have some path to reproducing or verifying the results.

5. Open access to data and code

Question: Does the paper provide open access to the data and code, with sufficient instructions to faithfully reproduce the main experimental results, as described in supplemental material?

Answer: **[Yes]**

Justification: Yes, we provide the data and code in supplementary materials, with sufficient instructions to reproduce the main experimental results.

Guidelines:

- The answer NA means that paper does not include experiments requiring code.
- Please see the NeurIPS code and data submission guidelines (<https://nips.cc/public/guides/CodeSubmissionPolicy>) for more details.
- While we encourage the release of code and data, we understand that this might not be possible, so “No” is an acceptable answer. Papers cannot be rejected simply for not including code, unless this is central to the contribution (e.g., for a new open-source benchmark).
- The instructions should contain the exact command and environment needed to run to reproduce the results. See the NeurIPS code and data submission guidelines (<https://nips.cc/public/guides/CodeSubmissionPolicy>) for more details.
- The authors should provide instructions on data access and preparation, including how to access the raw data, preprocessed data, intermediate data, and generated data, etc.
- The authors should provide scripts to reproduce all experimental results for the new proposed method and baselines. If only a subset of experiments are reproducible, they should state which ones are omitted from the script and why.
- At submission time, to preserve anonymity, the authors should release anonymized versions (if applicable).
- Providing as much information as possible in supplemental material (appended to the paper) is recommended, but including URLs to data and code is permitted.

6. Experimental setting/details

Question: Does the paper specify all the training and test details (e.g., data splits, hyper-parameters, how they were chosen, type of optimizer, etc.) necessary to understand the results?

Answer: **[Yes]**

Justification: Yes, we have provide all the training and test details in Section 5.1 and Appendix B.

Guidelines:

- The answer NA means that the paper does not include experiments.
- The experimental setting should be presented in the core of the paper to a level of detail that is necessary to appreciate the results and make sense of them.
- The full details can be provided either with the code, in appendix, or as supplemental material.

7. Experiment statistical significance

Question: Does the paper report error bars suitably and correctly defined or other appropriate information about the statistical significance of the experiments?

Answer: **[No]**

Justification: No previous work reports error bars.

Guidelines:

- The answer NA means that the paper does not include experiments.
- The authors should answer “Yes” if the results are accompanied by error bars, confidence intervals, or statistical significance tests, at least for the experiments that support the main claims of the paper.

- The factors of variability that the error bars are capturing should be clearly stated (for example, train/test split, initialization, random drawing of some parameter, or overall run with given experimental conditions).
- The method for calculating the error bars should be explained (closed form formula, call to a library function, bootstrap, etc.)
- The assumptions made should be given (e.g., Normally distributed errors).
- It should be clear whether the error bar is the standard deviation or the standard error of the mean.
- It is OK to report 1-sigma error bars, but one should state it. The authors should preferably report a 2-sigma error bar than state that they have a 96% CI, if the hypothesis of Normality of errors is not verified.
- For asymmetric distributions, the authors should be careful not to show in tables or figures symmetric error bars that would yield results that are out of range (e.g. negative error rates).
- If error bars are reported in tables or plots, The authors should explain in the text how they were calculated and reference the corresponding figures or tables in the text.

8. Experiments compute resources

Question: For each experiment, does the paper provide sufficient information on the computer resources (type of compute workers, memory, time of execution) needed to reproduce the experiments?

Answer: **[Yes]**

Justification: Yes, we provide sufficient information on computer resources needed to reproduce the experiments in Appendix B.2.

Guidelines:

- The answer NA means that the paper does not include experiments.
- The paper should indicate the type of compute workers CPU or GPU, internal cluster, or cloud provider, including relevant memory and storage.
- The paper should provide the amount of compute required for each of the individual experimental runs as well as estimate the total compute.
- The paper should disclose whether the full research project required more compute than the experiments reported in the paper (e.g., preliminary or failed experiments that didn't make it into the paper).

9. Code of ethics

Question: Does the research conducted in the paper conform, in every respect, with the NeurIPS Code of Ethics <https://neurips.cc/public/EthicsGuidelines>?

Answer: **[Yes]**

Justification: Yes, the authors have carefully reviewed the NeurIPS Code of Ethics, and the research in this paper conforms to the NeurIPS Code of Ethics.

Guidelines:

- The answer NA means that the authors have not reviewed the NeurIPS Code of Ethics.
- If the authors answer No, they should explain the special circumstances that require a deviation from the Code of Ethics.
- The authors should make sure to preserve anonymity (e.g., if there is a special consideration due to laws or regulations in their jurisdiction).

10. Broader impacts

Question: Does the paper discuss both potential positive societal impacts and negative societal impacts of the work performed?

Answer: **[NA]**

Justification: The proposed work focuses on Graph Edit Distance (GED), which is primarily a foundational research method aimed at improving the computational efficiency of graph similarity measurements. It is not specifically tied to real-world applications, and it does not directly involve any obvious negative social impact.

Guidelines:

- The answer NA means that there is no societal impact of the work performed.
- If the authors answer NA or No, they should explain why their work has no societal impact or why the paper does not address societal impact.
- Examples of negative societal impacts include potential malicious or unintended uses (e.g., disinformation, generating fake profiles, surveillance), fairness considerations (e.g., deployment of technologies that could make decisions that unfairly impact specific groups), privacy considerations, and security considerations.
- The conference expects that many papers will be foundational research and not tied to particular applications, let alone deployments. However, if there is a direct path to any negative applications, the authors should point it out. For example, it is legitimate to point out that an improvement in the quality of generative models could be used to generate deepfakes for disinformation. On the other hand, it is not needed to point out that a generic algorithm for optimizing neural networks could enable people to train models that generate Deepfakes faster.
- The authors should consider possible harms that could arise when the technology is being used as intended and functioning correctly, harms that could arise when the technology is being used as intended but gives incorrect results, and harms following from (intentional or unintentional) misuse of the technology.
- If there are negative societal impacts, the authors could also discuss possible mitigation strategies (e.g., gated release of models, providing defenses in addition to attacks, mechanisms for monitoring misuse, mechanisms to monitor how a system learns from feedback over time, improving the efficiency and accessibility of ML).

11. Safeguards

Question: Does the paper describe safeguards that have been put in place for responsible release of data or models that have a high risk for misuse (e.g., pretrained language models, image generators, or scraped datasets)?

Answer: [NA]

Justification: Our work does not involve the release of high-risk models, such as pretrained language models, image generators, or scraped datasets. Therefore, our paper poses no such risks.

Guidelines:

- The answer NA means that the paper poses no such risks.
- Released models that have a high risk for misuse or dual-use should be released with necessary safeguards to allow for controlled use of the model, for example by requiring that users adhere to usage guidelines or restrictions to access the model or implementing safety filters.
- Datasets that have been scraped from the Internet could pose safety risks. The authors should describe how they avoided releasing unsafe images.
- We recognize that providing effective safeguards is challenging, and many papers do not require this, but we encourage authors to take this into account and make a best faith effort.

12. Licenses for existing assets

Question: Are the creators or original owners of assets (e.g., code, data, models), used in the paper, properly credited and are the license and terms of use explicitly mentioned and properly respected?

Answer: [Yes]

Justification: The creators or original owners of assets used in the paper are properly credited and cited. The license and terms of use are properly respected.

Guidelines:

- The answer NA means that the paper does not use existing assets.
- The authors should cite the original paper that produced the code package or dataset.

- The authors should state which version of the asset is used and, if possible, include a URL.
- The name of the license (e.g., CC-BY 4.0) should be included for each asset.
- For scraped data from a particular source (e.g., website), the copyright and terms of service of that source should be provided.
- If assets are released, the license, copyright information, and terms of use in the package should be provided. For popular datasets, paperswithcode.com/datasets has curated licenses for some datasets. Their licensing guide can help determine the license of a dataset.
- For existing datasets that are re-packaged, both the original license and the license of the derived asset (if it has changed) should be provided.
- If this information is not available online, the authors are encouraged to reach out to the asset's creators.

13. New assets

Question: Are new assets introduced in the paper well documented and is the documentation provided alongside the assets?

Answer: [\[Yes\]](#)

Justification: Yes, new assets introduced in the paper are well documented, and a detailed documentation for the code is provided in the supplementary materials.

Guidelines:

- The answer NA means that the paper does not release new assets.
- Researchers should communicate the details of the dataset/code/model as part of their submissions via structured templates. This includes details about training, license, limitations, etc.
- The paper should discuss whether and how consent was obtained from people whose asset is used.
- At submission time, remember to anonymize your assets (if applicable). You can either create an anonymized URL or include an anonymized zip file.

14. Crowdsourcing and research with human subjects

Question: For crowdsourcing experiments and research with human subjects, does the paper include the full text of instructions given to participants and screenshots, if applicable, as well as details about compensation (if any)?

Answer: [\[NA\]](#)

Justification: The paper does not involve crowdsourcing nor research with human subjects.

Guidelines:

- The answer NA means that the paper does not involve crowdsourcing nor research with human subjects.
- Including this information in the supplemental material is fine, but if the main contribution of the paper involves human subjects, then as much detail as possible should be included in the main paper.
- According to the NeurIPS Code of Ethics, workers involved in data collection, curation, or other labor should be paid at least the minimum wage in the country of the data collector.

15. Institutional review board (IRB) approvals or equivalent for research with human subjects

Question: Does the paper describe potential risks incurred by study participants, whether such risks were disclosed to the subjects, and whether Institutional Review Board (IRB) approvals (or an equivalent approval/review based on the requirements of your country or institution) were obtained?

Answer: [\[NA\]](#)

Justification: The paper does not involve crowdsourcing nor research with human subjects.

Guidelines:

- The answer NA means that the paper does not involve crowdsourcing nor research with human subjects.
- Depending on the country in which research is conducted, IRB approval (or equivalent) may be required for any human subjects research. If you obtained IRB approval, you should clearly state this in the paper.
- We recognize that the procedures for this may vary significantly between institutions and locations, and we expect authors to adhere to the NeurIPS Code of Ethics and the guidelines for their institution.
- For initial submissions, do not include any information that would break anonymity (if applicable), such as the institution conducting the review.

16. Declaration of LLM usage

Question: Does the paper describe the usage of LLMs if it is an important, original, or non-standard component of the core methods in this research? Note that if the LLM is used only for writing, editing, or formatting purposes and does not impact the core methodology, scientific rigorousness, or originality of the research, declaration is not required.

Answer: [NA]

Justification: The core method development in this research does not involve LLMs as any important, original, or non-standard components.

Guidelines:

- The answer NA means that the core method development in this research does not involve LLMs as any important, original, or non-standard components.
- Please refer to our LLM policy (<https://neurips.cc/Conferences/2025/LLM>) for what should or should not be described.

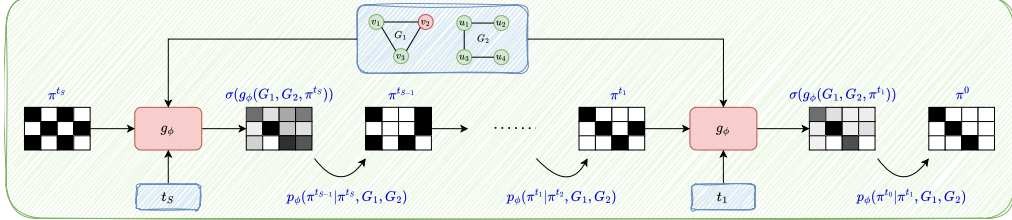


Figure 4: Reverse process of diffusion-based node matching model during inference.

Appendix

A Detailed Method

Algorithm 2 Reverse Process

Input: A pair of graphs (G_1, G_2) ;
1: $\pi^{t_s} \sim \text{Bernoulli}(0.5)^{|V_1| \times |V_2|}$;
2: **for** $i = S$ to 1 **do**
3: $p_\phi(\tilde{\pi}^0 | \pi^{t_i}, G_1, G_2) \leftarrow \sigma(g_\phi(G_1, G_2, \pi^{t_i}, t_i))$;
4: **if** $i \neq 1$ **then**
5: $\pi^{t_{i-1}} \sim p_\phi(\pi^{t_{i-1}} | \pi^{t_i}, G_1, G_2)$;
6: **else**
7: $\pi^0 \leftarrow \text{Greedy}(p_\phi(\pi^{t_{i-1}} | \pi^{t_i}, G_1, G_2))$;
8: **end if**
9: **end for**
10: **return** π^0 ;

Algorithm 3 GEDRanker Training Strategy

1: Initialize $\bar{\pi} \leftarrow \text{Greedy}(\hat{\pi})$, $\pi_{\text{last}} \leftarrow \text{Greedy}(\hat{\pi})$, with $\hat{\pi} \sim \mathcal{U}(0, 1)^{|V_1| \times |V_2|}$;
2: **for** each epoch **do**
3: Sample $t \sim \mathcal{U}(\{1, \dots, T\})$ and $\pi^t \sim q(\pi^t | \bar{\pi})$;
4: $\hat{\pi}_{g_\phi} \leftarrow S(g_\phi(G_1, G_2, \pi^t, t))$;
5: $\pi_{g_\phi} \leftarrow \text{Greedy}(\hat{\pi}_{g_\phi})$;
6: Compute $D_\theta(G_1, G_2, \hat{\pi}_{g_\phi})$, $D_\theta(G_1, G_2, \bar{\pi})$, $D_\theta(G_1, G_2, \pi_{\text{last}})$;
7: Compute \mathcal{L}_{D_θ} and update D_θ ;
8: Compute $D_\theta(G_1, G_2, \hat{\pi}_{g_\phi})$;
9: Compute \mathcal{L}_{g_ϕ} and update g_ϕ ;
10: **if** $c(G_1, G_2, \pi_{g_\phi}) < c(G_1, G_2, \bar{\pi})$ **then**
11: Update $\bar{\pi} \leftarrow \pi_{g_\phi}$;
12: **end if**
13: Update $\pi_{\text{last}} \leftarrow \pi_{g_\phi}$;
14: **end for**

A.1 Diffusion-based Node Matching Model Reverse Process

The detailed reverse process of diffusion-based node matching model is illustrated in Figure 4 and outlined in Algorithm 2.

A.2 GEDRanker

The detailed unsupervised training strategy of GEDRanker is outlined in Algorithm 3.

A.3 Network Architecture

Network Architecture of g_ϕ . The denoising network g_ϕ takes as input a graph pair (G_1, G_2) , a noisy matching matrix π^t , and the corresponding time step t , then predicts a matching score for each node pair. Intuitively, g_ϕ works by computing pair embedding of each node pair, followed by computing the matching score of each node pair based on its pair embedding.

Specifically, for each node $v \in V_1$ and $u \in V_2$, we initialize the node embeddings \mathbf{h}_v^0 and \mathbf{h}_u^0 as the one-hot encoding of their labels $L_1(v)$ and $L_2(u)$, respectively. For each node pair $(v, u) \in \pi^t$, we construct two directional pair embeddings \mathbf{h}_{vu}^0 and \mathbf{h}_{uv}^0 to ensure permutation invariance, since the input graph pair has no inherent order, i.e., $\text{GED}(G_1, G_2) = \text{GED}(G_2, G_1)$. Both \mathbf{h}_{vu}^0 and \mathbf{h}_{uv}^0 are initialized using the sinusodial embeddings [35] of $\pi^t[v][u]$. Moreover, the time step embedding \mathbf{h}_t is initialized as the sinusodial embedding of t .

Each layer l of g_ϕ consists of a two stage update. In the first stage, we independently update the node embeddings of each graph based on its own graph structure using siamese GIN [29] as follows:

$$\begin{aligned}\hat{\mathbf{h}}_v^l &= \text{GN}_{G_1}(\text{MLP}((1 + \epsilon^l) \cdot \mathbf{h}_v^{l-1} + \sum_{v' \in \mathcal{N}_{G_1}(v)} \mathbf{h}_{v'}^{l-1})) \\ \hat{\mathbf{h}}_u^l &= \text{GN}_{G_2}(\text{MLP}((1 + \epsilon^l) \cdot \mathbf{h}_u^{l-1} + \sum_{u' \in \mathcal{N}_{G_2}(u)} \mathbf{h}_{u'}^{l-1}))\end{aligned}\quad (10)$$

where ϵ^l is a learnable scalar, MLP denotes a multi-layer perceptron, GN_{G_1} and GN_{G_2} denote graph normalization [36] over G_1 and G_2 , respectively.

In the second stage, we simultaneously update the node embeddings of both graphs and the pair embeddings via Anisotropic Graph Neural Network (AGNN) [30, 31, 32], which incorporates the noisy interactions between node pairs and the corresponding time step t :

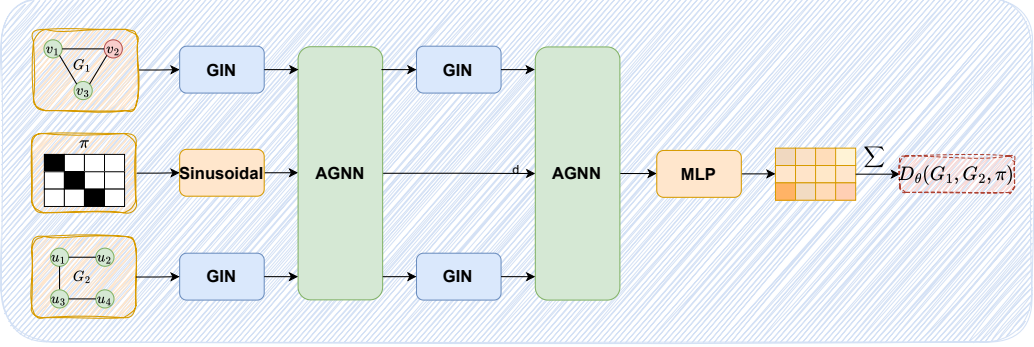
$$\begin{aligned}\hat{\mathbf{h}}_{vu}^l &= \mathbf{W}_1^l \mathbf{h}_{vu}^{l-1}, \quad \hat{\mathbf{h}}_{uv}^l = \mathbf{W}_1^l \mathbf{h}_{uv}^{l-1} \\ \tilde{\mathbf{h}}_{vu}^l &= \mathbf{W}_2^l \hat{\mathbf{h}}_{vu}^l + \mathbf{W}_3^l \hat{\mathbf{h}}_v^l + \mathbf{W}_4^l \hat{\mathbf{h}}_u^l \\ \tilde{\mathbf{h}}_{uv}^l &= \mathbf{W}_2^l \hat{\mathbf{h}}_{uv}^l + \mathbf{W}_3^l \hat{\mathbf{h}}_u^l + \mathbf{W}_4^l \hat{\mathbf{h}}_v^l \\ \mathbf{h}_{vu}^l &= \hat{\mathbf{h}}_{vu}^l + \text{MLP}(\text{ReLU}(\text{GN}_\pi(\tilde{\mathbf{h}}_{vu}^l)) + \mathbf{W}_5^l \mathbf{h}_t) \\ \mathbf{h}_{uv}^l &= \hat{\mathbf{h}}_{uv}^l + \text{MLP}(\text{ReLU}(\text{GN}_\pi(\tilde{\mathbf{h}}_{uv}^l)) + \mathbf{W}_5^l \mathbf{h}_t) \\ \mathbf{h}_v^l &= \hat{\mathbf{h}}_v^l + \text{ReLU}(\text{GN}_{G_1 G_2}(\mathbf{W}_6^l \hat{\mathbf{h}}_v^l + \sum_{u' \in V_2} \mathbf{W}_7^l \hat{\mathbf{h}}_{u'}^l \odot \sigma(\tilde{\mathbf{h}}_{vu'}^l))) \\ \mathbf{h}_u^l &= \hat{\mathbf{h}}_u^l + \text{ReLU}(\text{GN}_{G_1 G_2}(\mathbf{W}_6^l \hat{\mathbf{h}}_u^l + \sum_{v' \in V_1} \mathbf{W}_7^l \hat{\mathbf{h}}_{v'}^l \odot \sigma(\tilde{\mathbf{h}}_{uv'}^l)))\end{aligned}\quad (11)$$

where $\mathbf{W}_1^l, \mathbf{W}_2^l, \mathbf{W}_3^l, \mathbf{W}_4^l, \mathbf{W}_5^l, \mathbf{W}_6^l, \mathbf{W}_7^l$ are learnable parameters at layer l , GN_π denote the graph normalization over all node pairs and $\text{GN}_{G_1 G_2}$ denote the graph normalization over all nodes in both graphs G_1 and G_2 .

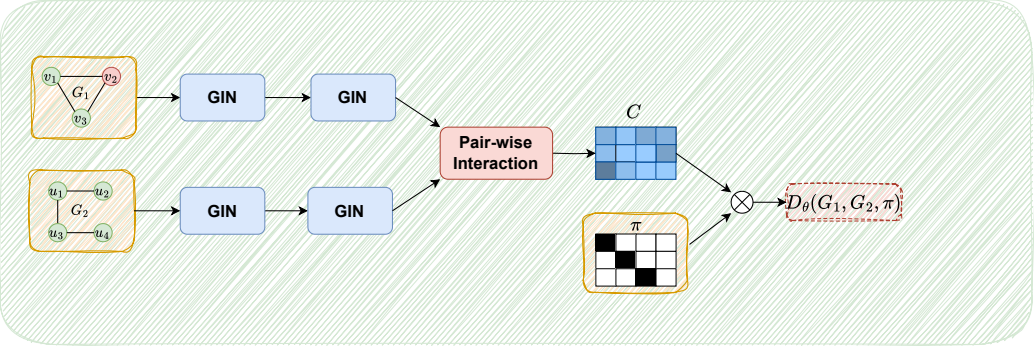
For a L -layer denoising network g_ϕ , the final matching score of each node pair is computed as follows:

$$g_\phi(G_1, G_2, \pi^t, t)[v][u] = \text{MLP}(\mathbf{h}_{vu}^L) + \text{MLP}(\mathbf{h}_{uv}^L) \quad (12)$$

Network Architecture of D_θ . The discriminator D_θ takes as input a graph pair (G_1, G_2) and a matching matrix π , then predicts a overall score for π . To better evaluate π , D_θ adopts the same structure as g_ϕ , which computes the embeddings of each node pair in π , and computes the overall score based on the pair embeddings. Specifically, computing the embeddings for each node pair enables D_θ to distinguish the influence of individual node pairs in π , while the use of AGNN allows D_θ to effectively capture complex dependencies between node pairs. An overview of D_θ 's network architecture is presented in Figure 5(a).



(a) Network architecture of D_θ in GEDRanker



(b) Network architecture of D_θ in GEDRanker (cost)

Figure 5: Comparison of D_θ ’s network architecture.

However, since D_θ does not include the time step t as an input, we remove the time step component from AGNN of the second update stage as follows:

$$\begin{aligned}
 \hat{\mathbf{h}}_{vu}^l &= \mathbf{W}_1^l \mathbf{h}_{vu}^{l-1}, \quad \hat{\mathbf{h}}_{uv}^l = \mathbf{W}_1^l \mathbf{h}_{uv}^{l-1} \\
 \tilde{\mathbf{h}}_{vu}^l &= \mathbf{W}_2^l \hat{\mathbf{h}}_{vu}^l + \mathbf{W}_3^l \hat{\mathbf{h}}_v^l + \mathbf{W}_4^l \hat{\mathbf{h}}_u^l \\
 \tilde{\mathbf{h}}_{uv}^l &= \mathbf{W}_2^l \hat{\mathbf{h}}_{uv}^l + \mathbf{W}_3^l \hat{\mathbf{h}}_u^l + \mathbf{W}_4^l \hat{\mathbf{h}}_v^l \\
 \mathbf{h}_{vu}^l &= \hat{\mathbf{h}}_{vu}^l + \text{MLP}(\text{ReLU}(\text{GN}_\pi(\tilde{\mathbf{h}}_{vu}^l))) \\
 \mathbf{h}_{uv}^l &= \hat{\mathbf{h}}_{uv}^l + \text{MLP}(\text{ReLU}(\text{GN}_\pi(\tilde{\mathbf{h}}_{uv}^l))) \\
 \mathbf{h}_v^l &= \hat{\mathbf{h}}_v^l + \text{ReLU}(\text{GN}_{G_1 G_2}(\mathbf{W}_6^l \hat{\mathbf{h}}_v^l + \sum_{u' \in V_2} \mathbf{W}_7^l \hat{\mathbf{h}}_{u'}^l \odot \sigma(\tilde{\mathbf{h}}_{vu'}^l))) \\
 \mathbf{h}_u^l &= \hat{\mathbf{h}}_u^l + \text{ReLU}(\text{GN}_{G_1 G_2}(\mathbf{W}_6^l \hat{\mathbf{h}}_u^l + \sum_{v' \in V_1} \mathbf{W}_7^l \hat{\mathbf{h}}_{v'}^l \odot \sigma(\tilde{\mathbf{h}}_{uv'}^l)))
 \end{aligned} \tag{13}$$

For a L -layer discriminator D_θ , the overall score of π is computed as follows:

$$D_\theta(G_1, G_2, \pi) = \sum_{(v, u) \in \pi} (\text{MLP}(\mathbf{h}_{vu}^L) + \text{MLP}(\mathbf{h}_{uv}^L)) \tag{14}$$

A.4 Alternative Ranking Loss

Hinge Loss. Hinge loss could be an alternative ranking loss for our preference-aware discriminator. At each training step, for a pair of graphs, given the current best node matching matrix $\bar{\pi}$ and the

predicted $\hat{\pi}_{g_\phi}$, the discriminator can be trained to minimize the following Hinge loss:

$$\mathcal{L}_{Hinge}(\hat{\pi}_{g_\phi}, \bar{\pi}) = \begin{cases} \max(0, D_\theta(G_1, G_2, \bar{\pi}) - D_\theta(G_1, G_2, \hat{\pi}_{g_\phi}) + \text{margin}) & \text{if } c(G_1, G_2, \hat{\pi}_{g_\phi}) \leq c(G_1, G_2, \bar{\pi}) \\ \max(0, D_\theta(G_1, G_2, \hat{\pi}_{g_\phi}) - D_\theta(G_1, G_2, \bar{\pi}) + \text{margin}) & \text{if } c(G_1, G_2, \hat{\pi}_{g_\phi}) \geq c(G_1, G_2, \bar{\pi}) \end{cases} \quad (15)$$

where margin is set to 0 if $c(G_1, G_2, \hat{\pi}_{g_\phi}) = c(G_1, G_2, \bar{\pi})$, otherwise 1.

B Experimental Setting

B.1 Dataset

We conduct experiments on three widely used real world datasets: AIDS700 [17], Linux [33, 17], and IMDB [17, 34]. Table 3 shows the statistics of the datasets. For each dataset, we split into 60%, 20% and 20% as training graphs, validation graphs and testing graphs, respectively.

To construct training graph pairs, all training graphs with no more than 10 nodes are paired with each other. For these small graph pairs, the ground-truth GEDs and node matching matrices are obtained using the exact algorithm. For graph pairs with more than 10 nodes, ground-truth labels are infeasible to obtain, we follow the strategy described in [11] to generate 100 synthetic graphs for each training graph with more than 10 nodes. Specifically, for a given graph, we apply Δ random edit operations to it, where Δ is randomly distributed in $[1, 10]$ for graphs with more than 20 nodes, and is randomly distributed in $[1, 5]$ for graphs with no more than 20 nodes. Δ is used as an approximation of the ground-truth GED.

To form the validation/testing graph pairs, each validation/testing graph with no more than 10 nodes is paired with 100 randomly selected training graphs with no more than 10 nodes. And each validation/testing graph with more than 10 nodes is paired with 100 synthetic graphs.

Table 3: Dataset statistics.

Dataset	# Graphs	Avg $ V $	Avg $ E $	Max $ V $	Max $ E $	Number of Labels
AIDS700	700	8.9	8.8	10	14	29
Linux	1000	7.6	6.9	10	13	1
IMDB	1500	13	65.9	89	1467	1

B.2 Implementation Details

Network. The denoising network g_ϕ consists of 6 layers with output dimensions $[128, 64, 32, 32, 32, 32]$, while the discriminator D_θ consists of 3 layers with output dimensions $[128, 64, 32]$.

Training. During training, the number of time steps T for the forward process is set to 1000 with a linear noise schedule, where $\beta_0 = 10^{-4}$ and $\beta_T = 0.02$. For the Gumbel-Sinkhorn operator, the number of iterations K is set to 5 and the temperature τ is set to 1. Moreover, we train g_ϕ and D_θ for 200 epochs with a batch size of 128. The loss weight λ for $\mathcal{L}_{\text{explore}}$ in \mathcal{L}_{g_ϕ} (Equation 6) is linearly annealed from 1 to 0 during the first 100 epochs, and fixed at 0 for the remaining 100 epochs. For the optimizer, We adopt RMSProp with a learning rate of 0.001 and a weight decay of 5×10^{-4} .

Inference. During inference, the number of time steps S for the reverse process is set to 10 with a linear denoising schedule. For each test graph pair, we generate $k = 100$ candidate node matching matrices in parallel.

Testbed. All experiments are performed using an NVIDIA GeForce RTX 3090 24GB and an Intel Core i9-12900K CPU with 128GB RAM.

Table 4: Overall performance on unseen testing graph pairs.

Datasets	Models	Type	MAE \downarrow	Accuracy \uparrow	$\rho \uparrow$	$\tau \uparrow$	$p@10 \uparrow$	$p@20 \uparrow$	Time(s) \downarrow
AIDS700	Hungarian	Trad	8.237	1.5%	0.527	0.416	54.3%	60.3%	0.0001
	VJ	Trad	14.171	0.9%	0.391	0.302	44.9%	52.9%	0.00016
	GEDGW	Trad	0.828	53%	0.85	0.764	86.4%	85.8%	0.38911
	Noah	SL	3.174	6.8%	0.735	0.617	77.8%	76.4%	0.5765
	GENN-A*	SL	0.508	67.1%	0.917	0.836	87.1%	90.6%	3.44326
	MATA*	SL	0.885	56.6%	0.77	0.689	73.2%	76.6%	0.00486
Linux	GEDGNN	SL	1.155	50.5%	0.838	0.746	89.1%	87.6%	0.39344
	GEDIOT	SL	1.348	47.4%	0.81	0.71	88.4%	86.9%	0.39707
	DiffGED	SL	0.024	96.4%	0.993	0.986	99.7%	99.7%	0.07546
	GEDRanker (Ours)	UL	0.101	91.4%	0.981	0.963	99%	99%	0.07616
	Hungarian	Trad	5.423	7.5%	0.725	0.623	75%	77%	0.00008
	VJ	Trad	11.174	0.4%	0.613	0.512	70.6%	74.5%	0.00013
IMDB	GEDGW	Trad	0.568	73.5%	0.925	0.865	90.9%	91.5%	0.17768
	Noah	SL	1.879	8%	0.872	0.796	84.3%	92.2%	0.25712
	GENN-A*	SL	0.142	92.9%	0.976	0.94	99.6%	99.6%	1.17702
	MATA*	SL	0.201	91.5%	0.948	0.903	86.2%	90.2%	0.00464
	GEDGNN	SL	0.105	96.2%	0.979	0.968	98.6%	98.5%	0.12169
	GEDIOT	SL	0.14	94.8%	0.973	0.959	98.1%	98.3%	0.12826
IMDB	DiffGED	SL	0.0	100%	1.0	1.0	100%	100%	0.06901
	GEDRanker (Ours)	UL	0.008	99.6%	0.998	0.997	99.5%	99.7%	0.07065
	Hungarian	Trad	21.156	45.9%	0.776	0.717	84.2%	82.1%	0.00012
	VJ	Trad	44.072	26.6%	0.4	0.359	60.1%	63.1%	0.00037
	GEDGW	Trad	0.349	93.9%	0.966	0.953	99.2%	98.3%	0.37384
	Noah	SL	-	-	-	-	-	-	-
IMDB	GENN-A*	SL	-	-	-	-	-	-	-
	MATA*	SL	-	-	-	-	-	-	-
	GEDGNN	SL	2.484	85.5%	0.895	0.876	92.3%	91.7%	0.42662
	GEDIOT	SL	2.83	84.4%	0.989	0.876	92.5%	92.4%	0.42269
	DiffGED	SL	0.932	94.6%	0.982	0.974	97.5%	98.4%	0.15107
	GEDRanker (Ours)	UL	1.025	93.9%	0.998	0.968	96%	97%	0.15012

C More Experimental Results

C.1 Generalization Ability

To evaluate the generalization ability of GEDRanker, we construct testing graph pairs by pairing each testing graph with 100 unseen testing graphs, instead of with training graphs. The overall performance on these unseen pairs is reported in Table 4. On unseen testing pairs, our unsupervised GEDRanker continues to achieve near-optimal performance, with only a marginal gap compared to the supervised DiffGED, and consistently outperforms all other supervised and traditional baselines. Furthermore, compared to the results in Table 1, there is no significant performance drop, demonstrating the generalization ability of our GEDRanker.

C.2 Scalability

Table 5: Overall performance on large testing graph pairs.

Datasets	Models	Average GED \downarrow	Time(s) \downarrow
IMDB-large	Hungarian	234.656	0.00016
	VJ	219.465	0.00039
	GEDGW	140.278	0.4032
	DiffGED (small)	143.607	0.1911
GEDRanker (Ours)		140.138	0.1904

Table 6: Ablation study on D_θ 's network architecture.

Datasets	Models	MAE \downarrow	Accuracy \uparrow	$\rho \uparrow$	$\tau \uparrow$	$p@10 \uparrow$	$p@20 \uparrow$
AIDS700	GEDRanker (cost)	0.528	66.3%	0.907	0.841	90.4%	92%
	GEDRanker	0.088	92.6%	0.984	0.969	99.1%	99.1%
Linux	GEDRanker (cost)	0.102	94.9%	0.98	0.965	96.8%	97.1%
	GEDRanker	0.01	99.5%	0.997	0.995	100%	99.8%

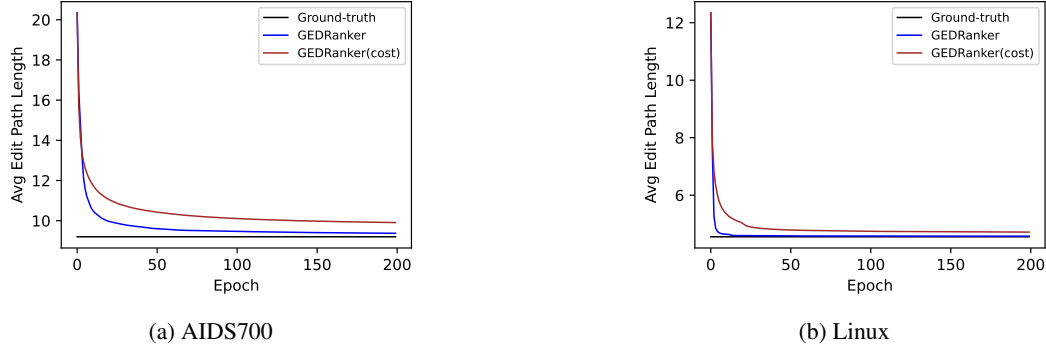


Figure 6: Impact of D_θ 's network architecture on the average edit path length of the best found node matching matrices on training graph pairs.

To evaluate the scalability of GEDRanker, we construct training pairs by pairing each large training graph in the IMDB dataset with all other large training graphs, instead of using synthetic graphs. For testing, we form pairs by pairing each large testing graph with 100 large training graphs. Since the scalability of GEDRanker can be inherently influenced by the base model, DiffGED. Therefore, an appropriate way to demonstrate our method's effectiveness on large graphs is to evaluate how it enhances the scalability of the base model in practice. To do so, we train the base model (DiffGED) only on small real-world IMDB graph pairs where ground-truth labels are available, then evaluate on the large testing graph pairs to see the scalability of the original base model, and compare with our GEDRanker that enables the training of base model on large graph pairs without requiring ground-truth supervision. For a clear reference, we also compare with traditional methods, and we report the average estimated GED across all testing pairs, along with the average inference time per testing pair.

Table 5 summarizes the overall performance of each method. Under this practical setting, we can see that the supervised DiffGED underperforms the optimization algorithm GEDGW in terms of average GED. However, by leveraging our unsupervised training strategy (GEDRanker), DiffGED can be trained on large graphs and subsequently outperforms GEDGW in both average GED and running time, highlighting its scalability.

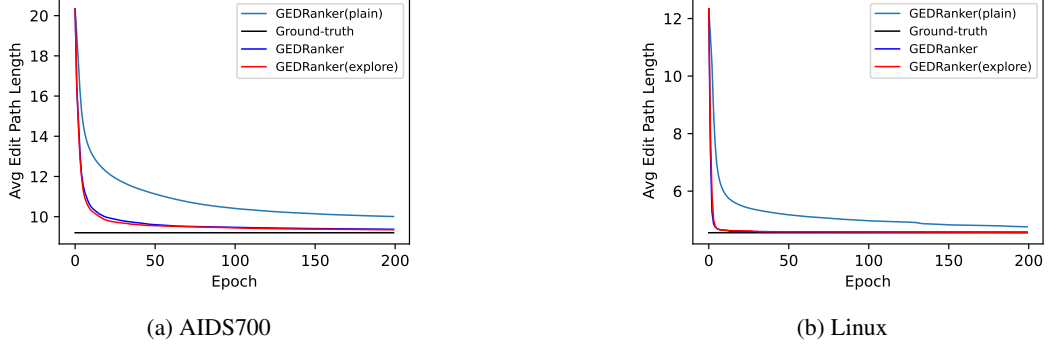
C.3 Ablation Study on the Network Architecture of D_θ

To evaluate the impact of D_θ 's network architecture on the performance of GEDRanker, we create a variant model, *GEDRanker (cost)*, that adopts an alternative network design inspired by typical architectures used in regression-based GED estimation [11, 12]. Figure 5(b) shows an overview of the network architecture of D_θ in GEDRanker (cost).

Specifically, given a graph pair (G_1, G_2) and a node matching matrix π , we compute nodes embeddings using GIN. Based on the pairwise node interactions, we then construct a matching cost matrix $C \in \mathbb{R}^{|V_1| \times |V_2|}$. Finally, the score $D_\theta(G_1, G_2, \pi)$ is estimated by $\langle \pi, C \rangle$. The overall architecture of D_θ can be represented as follows:

Table 7: Ablation study on loss weight λ .

Datasets	Models	MAE \downarrow	Accuracy \uparrow	$\rho \uparrow$	$\tau \uparrow$	$p@10 \uparrow$	$p@20 \uparrow$
AIDS700	GEDRanker (plain)	0.549	65.4%	0.905	0.837	91.7%	91.5%
	GEDRanker (explore)	1.334	39.3%	0.789	0.689	76.5%	79.9%
	GEDRanker	0.088	92.6%	0.984	0.969	99.1%	99.1%
Linux	GEDRanker (plain)	0.079	96.2%	0.984	0.973	98.1%	98.3%
	GEDRanker (explore)	0.146	93.4%	0.973	0.955	96.6%	98.2%
	GEDRanker	0.01	99.5%	0.997	0.995	100%	99.8%


Figure 7: Impact of λ 's network architecture on the average edit path length of the best found node matching matrices on training graph pairs.

$$\begin{aligned}
\mathbf{h}_v^l &= \text{GN}_{G_1}(\text{MLP}((1 + \epsilon^l) \cdot \mathbf{h}_v^{l-1} + \sum_{v' \in \mathcal{N}_{G_1}(v)} \mathbf{h}_{v'}^{l-1})) \\
\mathbf{h}_u^l &= \text{GN}_{G_2}(\text{MLP}((1 + \epsilon^l) \cdot \mathbf{h}_u^{l-1} + \sum_{u' \in \mathcal{N}_{G_2}(u)} \mathbf{h}_{u'}^{l-1})) \\
\mathbf{H}_1 &= [\mathbf{h}_v^L]_{v \in V_1}, \quad \mathbf{H}_2 = [\mathbf{h}_u^L]_{u \in V_2} \\
\mathbf{C} &= \text{MLP}([\mathbf{H}_1 \mathbf{W}_1 \mathbf{H}_2^\top, \mathbf{H}_1 \mathbf{W}_2 \mathbf{H}_2^\top, \dots, \mathbf{H}_1 \mathbf{W}_n \mathbf{H}_2^\top]) \\
D_\theta(G_1, G_2, \pi) &= \langle \pi, \mathbf{C} \rangle
\end{aligned} \tag{16}$$

where we set $L = 3$ and $n = 16$.

Table 6 shows the overall performance of GEDRanker (cost). Surprisingly, GEDRanker (cost) performs significantly worse than GEDRanker. This phenomenon can be attributed to the following reasons: (1) Although GEDRanker (cost) estimates the score by assigning each node pair in π an individual cost from \mathbf{C} , these costs are fixed for each node pair, irrespective of the actual value in π . The final score is computed as a simple linear combination $\langle \pi, \mathbf{C} \rangle$, which neglects the complex dependencies and interactions among node pairs. In contrast, D_θ in our GEDRanker directly computes node pair embeddings conditioned on the value in π , and leverages AGNN to capture interactions among node pairs; (2) The node matching matrix π is inherently sparse, with most of its elements being 0. This sparsity significantly limits the ability of D_θ to learn correct \mathbf{C} as only a few nonzero elements contribute to gradient updates. In contrast, D_θ in our GEDRanker transforms each value in π into embeddings that enables effective gradient updates even the value is 0 in π .

Consequently, D_θ in GEDRanker (cost) struggles to estimate the correct preference order over different π , thereby misguiding g_ϕ 's exploration direction, as demonstrated in Figure 6. This ultimately results in inferior performance.

C.4 Ablation Study on Loss Weight λ

In our GEDRanker, g_ϕ is trained to minimize $\mathcal{L}_{g_\phi} = \mathcal{L}_{\text{rec}(\bar{\pi})} + \lambda \mathcal{L}_{\text{explore}}$, where the loss weight λ is dynamically annealed during training to prioritize exploration in the early stages and shift g_ϕ 's

Table 8: Ablation study on the decay schedule of λ .

Decay Schedule	Datasets	MAE \downarrow	Accuracy \uparrow	$\rho \uparrow$	$\tau \uparrow$	$p@10 \uparrow$	$p@20 \uparrow$
Linear	AIDS	0.088	92.6%	0.984	0.969	99.1%	99.1%
	Linux	0.01	99.5%	0.997	0.995	100%	99.8%
Cosine	AIDS	0.130	90.2%	0.977	0.955	99.2%	98.9%
	Linux	0.012	99.4%	0.996	0.994	99.8%	99.7%
Step	AIDS	0.095	91.7%	0.981	0.963	99.0%	99.2%
	Linux	0.013	99.4%	0.996	0.994	99.9%	99.7%

focus toward recovering high-quality (exploitation) in the later stages. In Section 5.3, we evaluated GEDRanker (plain), which trains g_ϕ without any exploration by setting $\lambda = 0$. To understand the impact of prioritizing exploration through the entire training process, we create a variant model, *GEDRanker (explore)*, where λ is fixed at 1.

Table 7 compares the performance of GEDRanker under different settings of λ . It is unexpected to observe that GEDRanker (explore) performs extremely poorly on the AIDS700 dataset. Although GEDRanker (explore) demonstrates strong exploration ability comparable to GEDRanker, as illustrated in Figure 7, its performance is still significantly worse.

The reason for this phenomenon lies in the mismatch between the training objective and the reverse diffusion process during inference. In a standard diffusion model, the reverse process is designed to gradually remove noise from the noisy node matching matrix step by step through a Markov chain (see Equation 2). During this process, g_ϕ is expected to correctly remove the noise from π^t . However, GEDRanker (explore) prioritizes exploration throughout the entire training process. This excessive focus on exploration prevents g_ϕ from learning the essential noise-removal patterns required by the reverse process. Although g_ϕ might still output high-quality node matching probability matrices at some steps, it still disrupts the reverse diffusion path, causing significant misalignment with the expected denoising trajectory. Consequently, errors are accumulated during reverse process, leading to inferior performance.

In contrast, our GEDRanker dynamically decreases λ during training, promoting strong exploration in the early stages, while gradually shifting focus toward effective denoising of π^t in alignment with the reverse diffusion process. This balanced strategy enables both thorough exploration during training and high-quality solutions during inference.

C.5 Ablation Study on the Decay Schedule of λ

For GEDRanker, we adopt a linear decay schedule for λ . To investigate the impact of different decay strategies, we further experiment with cosine decay and step decay: (1) Cosine decay provides a similarly smooth transition as linear decay. Compared with the linear scheduler, it assigns more weight to exploration during the early stages and reduces the exploration weight more aggressively in the later stages. (2) Step decay maintains $\lambda = 1$ throughout the entire exploration phase and then directly drops it to 0 for exploitation.

As shown in Table 8, the performance of GEDRanker under different decay schedules exhibits no significant gap, indicating that our method is effective and robust without relying on complex scheduling strategies.

C.6 Compatibility

Our unsupervised training method is not limited to DiffGED and can be easily integrated with other hybrid matching-based frameworks. To demonstrate the compatibility of GEDRanker, we integrate it with GEDGNN. As shown in Table 9, GEDGNN trained with our unsupervised method achieves performance comparable to that of GEDGNN trained with supervision, highlighting both the effectiveness and compatibility of our approach.

Table 9: Performance of GEDGNN trained with our unsupervised method.

Setting	Datasets	MAE \downarrow	Accuracy \uparrow	$\rho \uparrow$	$\tau \uparrow$	$p@10 \uparrow$	$p@20 \uparrow$
Supervised	AIDS	1.098	52.5%	0.845	0.752	89.1%	88.3%
	Linux	0.094	96.6%	0.979	0.969	98.9%	99.3%
	IMDB	2.469	85.5%	0.898	0.879	92.4%	92.1%
Unsupervised	AIDS	1.279	44.6%	0.809	0.712	82.6%	83.7%
	Linux	0.078	96.3%	0.982	0.971	98.2%	98.7%
	IMDB	2.536	85.2%	0.896	0.876	92.0%	91.9%

D Discussion of Limitations

Although GEDRanker has demonstrated promising results on the three most commonly used real-world GED datasets, one notable limitation of this paper is that, for pairs of larger graphs, obtaining ground-truth GED values becomes infeasible. As a result, we can only evaluate the differences in estimated GED values among baseline methods, rather than the actual gap between the estimated GED values and the real GED values. This also prevents us from evaluating ranking-based metrics for each test query graph in such scenarios.